

Building high-performance integrated optical devices using subwavelength grating metamaterials

Alejandro Sánchez-Postigo^{1,*}, Pablo Ginel-Moreno¹, Alejandro Ortega-Moñux¹, J. Gonzalo Wangüemert-Pérez¹, Robert Halir¹, Daniel Pereira-Martín¹, Abdelfettah Hadij-ElHouati¹, Jens H. Schmid², Shurui Wang², Martin Vachon², Dan-Xia Xu², Winnie N. Ye³, Jordi Soler Penadés^{4,5}, Milos Nedeljkovic⁴, Goran Z. Mashanovich⁴, Pavel Cheben², and Íñigo Molina-Fernández¹

¹Universidad de Málaga, Dpto. Ingeniería de Comunicaciones, ETSI Telecomunicación, 29071 Málaga, Spain

²National Research Council Canada, 1200 Montreal Road, Bldg. M50, Ottawa, Ontario K1A 0R6, Canada

³Department of Electronics, Carleton University, 1125 Colonel By Drive, Ottawa, Ontario K1S5B6, Canada

⁴Optoelectronics Research Centre, University of Southampton, Southampton, SO17 1BJ, United Kingdom

⁵Currently at VLC Photonics S.L., Valencia, Spain

Abstract. The use of subwavelength grating structures in silicon waveguides have fuelled the development of integrated optical components with superior performance. By a judicious lithographic pattern of the grating, the optical properties of the synthesized metamaterial can be accurately tailored. In this work, we review our latest advances in subwavelength-grating-engineered silicon and germanium planar devices.

1 Introduction

Subwavelength grating (SWG) metamaterials are becoming established as an advantageous tool to manipulate light in integrated photonic devices [1,2]. SWG nanophotonic waveguides comprise an arrangement of structures with a period that is smaller than half the effective wavelength. The optical properties of the waveguide, including refractive index contrast and wavelength dispersion, can be controlled by choosing the geometrical parameters of the lithographically defined patterns. In this work, we leverage the refractive-index engineering possibilities of SWG metamaterials to implement high-performance waveguide-based devices for the near- and mid-infrared wavelength ranges.

2 Broadband surface grating couplers with sub-decibel coupling efficiency

Efficient and broadband fibre-to-chip coupling is a major challenge in silicon photonics [3]. Surface grating couplers are often used, as they allow wafer scale-testing and provide robust misalignment tolerances. The two important parameters in surface grating couplers are the coupling efficiency and the 1-dB bandwidth. For a given fibre mode field diameter, there is a trade-off between these two parameters and the coupling efficiency–bandwidth product (CE·BW) is an important figure of merit. We have shown how to break the coupling efficiency–bandwidth product limit of surface grating couplers by using subwavelength grating (SWG) metamaterials to radiate in the zeroth diffraction order [4].

Our proposed coupler, illustrated in Fig. 1, is formed by a subwavelength grating waveguide and a silicon prism on top with a tilt angle ϕ_{clad} , leaving a wedge-shaped air gap with initial thickness t_0 . The light injected into the grating from an input waveguide is evanescently coupled to the prism and then into an SMF-28 optical fibre via an anti-reflection coated facet. The metamaterial refractive index is engineered to optimize the bandwidth, while the angle ϕ_{clad} and the thickness t_0 are chosen to maximize the coupling efficiency. A two-stage transition at the beginning of the grating adapts the fundamental mode of the input waveguide to the Bloch mode of the grating.

Using the zero-order grating coupler, we achieve experimentally a coupling efficiency < 1 dB and a 1-dB bandwidth of 94 nm, yielding a CE·BW product exceeding 75 nm, the highest performance yet reported for a silicon photonics surface grating coupler.

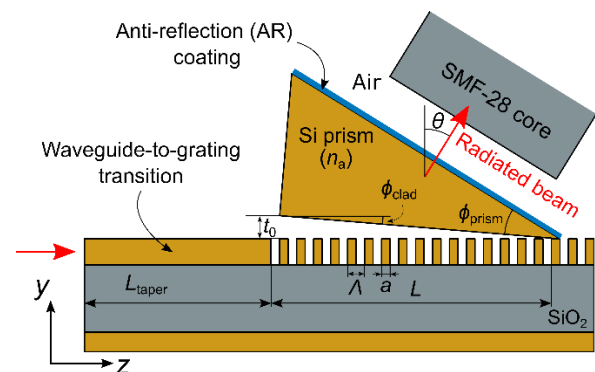


Fig. 1. Schematic of a zero-order fiber-chip coupler (side view).

* Corresponding author: asp@ic.uma.es

3 Millimetre-long optical antennas with DUV-compatible feature sizes

The rising need for compact, lightweight, and inexpensive light detection and ranging (LiDAR) systems and free-space communication transceivers has fuelled research in silicon photonics optical phased arrays (OPAs). Integrated optical antennas are the key components of OPAs and can be designed to enable rapid, precise, and non-mechanical steering of optical beams.

We have reported on a millimetre-long silicon optical antenna composed of an SWG waveguide core that is loaded with evanescently coupled radiative elements [5]. The SWG metamaterial allows us to delocalize the propagating mode to accurately control the radiation strength. Our experiments confirm a record beamwidth of $\sim 0.1^\circ$ for a minimum feature size of 80 nm and a wavelength sensitivity of $\sim 0.13^\circ/\text{nm}$.

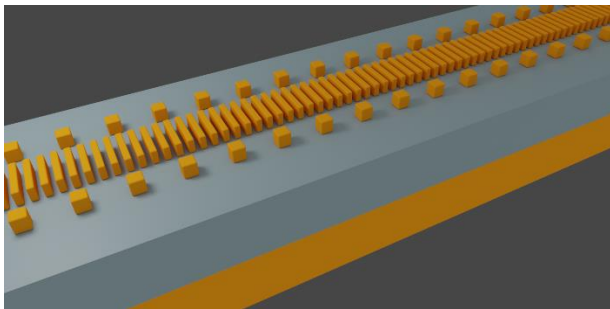


Fig. 3. 3D schematic view of a millimetre-long optical antenna with SWG waveguide core and evanescently coupled loading segments.

4 Suspended germanium waveguide platform for the longwave infrared band

The longwave infrared band has attracted great attention for important emerging applications such as biochemical sensing and free-space optical communications. The high material losses of silicon dioxide and silicon above wavelengths of $\sim 4 \mu\text{m}$ and $\sim 8 \mu\text{m}$, respectively, prevent the use of the SOI platform in the longwave range. Germanium, a CMOS-compatible semiconductor that is transparent up to $\sim 15\text{-}\mu\text{m}$ wavelength, can be used to develop waveguide-based devices at long wavelengths.

We have recently demonstrated a suspended germanium platform, based on Ge-on-SOI, operating at a wavelength of $7.7 \mu\text{m}$ [6]. The waveguide is defined by etching a subwavelength-grating cladding that anchors the waveguide core to lateral slabs. This cladding synthesizes a metamaterial that is judiciously engineered to provide the lateral index contrast required for light guiding. The buried silicon and silicon-dioxide layers of the Ge-on-SOI wafer are removed by a hydrofluoric (HF) acid solution, which flows through the venting holes of the subwavelength-grating cladding. Figure 3 shows an SEM image of one of the fabricated suspended waveguides. At a wavelength of $7.7 \mu\text{m}$, we measured a propagation loss of $5.3 \pm 1.0 \text{ dB/cm}$. Furthermore, by simulation we have confirmed that the proposed platform can be adapted to operate with low loss up to a wavelength of $15 \mu\text{m}$.

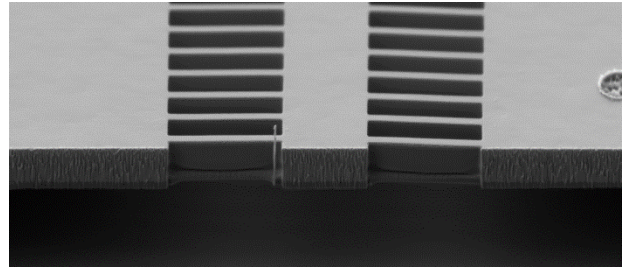


Fig. 3. Scanning electron micrograph of a suspended germanium waveguide designed to operate at a wavelength of $7.7 \mu\text{m}$.

To couple light into the suspended germanium waveguides from a commercially available, high-numerical-aperture chalcogenide optical fibre, we utilized suspended micro-antennas [7]. These couplers exhibit a respectable coupling efficiency of $\sim 40\%$, a broad 1-dB spectral bandwidth in excess of 430 nm, and a 1-dB angular bandwidth of $\sim 20^\circ$.

These results demonstrate the practical use of subwavelength-grating metamaterials in the longwave infrared regime.

We acknowledge funding from Universidad de Málaga, Ministerio de Ciencia, Innovación y Universidades (MCIU) (PID2019-106747RB-I00), Consejería de Economía, Conocimiento, Empresas y Universidad (CECEU) (UMA18-FEDERJA-219, P18-RT-1453, P18-RT-793) and National Research Council of Canada (NRC) Collaborative Science, Technology and Innovation Program (CSTIP) (HTSN 209).

References

1. P. Cheben, R. Halir, J. H. Schmid, H. A. Atwater, and D. R. Smith, *Nature* **560**, 565–572 (2018).
2. R. Halir, A. Ortega-Moñux, D. Benedikovic, G. Z. Mashanovich, J. G. Wangüemert-Pérez, J. H. Schmid, Í. Molina-Fernández, and P. Cheben, *Proc. IEEE* **106**,
3. R. Marchetti, C. Lacava, L. Carroll, K. Gradkowski, and P. Minzioni, *Photonics Res.* **7**, 201–239 (2019).
4. A. Sánchez-Postigo, R. Halir, J. G. Wangüemert-Pérez, A. Ortega-Moñux, S. Wang, M. Vachon, J. H. Schmid, D. Xu, P. Cheben, and Í. Molina-Fernández, *Laser Photon. Rev.* 2000542 (2021).
5. P. Ginel-Moreno, D. Pereira-Martín, A. Hadji-EiHouati, W. N. Ye, D. Melati, D.-X. Xu, S. Janz, A. Ortega-Moñux, J. G. Wangüemert-Pérez, R. Halir, Í. Molina-Fernández, J. H. Schmid, and P. Cheben, *Opt. Lett.* **45**, 5668–5671 (2020).
6. A. Sánchez-Postigo, A. Ortega-Moñux, J. Soler Penades, A. Osman, M. Nedeljkovic, Z. Qu, Y. Wu, I. Molina-Fernández, P. Cheben, G. Mashanovich, and J. G. Wangüemert-Pérez, *Opt. Express* **29** (2021).
7. A. Sánchez-Postigo, A. Ortega-Moñux, D. Pereira-Martín, Í. Molina-Fernández, R. Halir, P. Cheben, J. Soler Penades, M. Nedeljkovic, G. Z. Mashanovich, and J. G. Wangüemert-Pérez, *Opt. Express* **27**, 22302–22315 (2019).